The 15th International Symposium on Magnetic Bearings, August 3-6, 2016, Mojiko Hotel, Kitakyushu, Japan

ISMB15

Thermal model for a low-speed flywheel in low vacuum

Virginie KLUYSKENS*, Maxence VAN BENEDEN* and Bruno DEHEZ*

* Center for Research in Mechatronics, IMMC, Universite Catholique de Louvain

Place du Levant 2 bte L5.04.02, 1348 Louvain-la-Neuve, Belgium

E-mail: virginie.kluyskens@uclouvain.be

Abstract

This paper presents a model aimed to predict the temperature inside a flywheel energy storage system, and more specifically the temperature of the permanent magnet bearings of the system. The windage losses are evaluated by supposing an incompressible Couette flow between the flywheel and the enclosure. The eddy current losses inside the permanent magnet bearing are evaluated by a finite element (FE) electro-mechanical model. Those losses are injected into a FE thermal model. It shows that, in stationary low vacuum conditions, the temperature remains at acceptable levels. The sensitivity of the model to various parameters is also studied. Finally, the case of a loss of vacuum is examined, and it is shown that the system has a high time constant, and that the temperature of the magnets raises slowly enough.

Key words : Permanent Magnet Bearing, Flywheel, Thermal Model, Windage losses.

1. Introduction

Flywheel energy storage systems (FESS) appears to be a good solution for storing energy for high to medium power applications and for short or medium term storage (Sabihuddin et al.,2015). The advantages of FESS are a high number of cycles, and a state of charge directly related to the spin speed of the system, which means an easy monitoring.
Usually FESS include magnetic bearings (Genta, 2014) and an enclosure allowing to work at low pressure. These two elements allow a reduction of the losses in the system, friction losses for the first and windage losses for the second, in order to reach lower self-discharge rates.

However, losses are still present in the system, and the evacuation of these losses might be problematic as the flywheel is working in a low pressure environment.
When the design of the flywheel results in a system with permanent magnet bearings (Van Beneden et al., 2015), the operation temperature is a major input for the sizing of this bearing. Indeed the remanent magnetic flux density of the permanent magnets depends on this temperature (Friebe and Zacharias, 2014) and the degradation of the performances of the magnets for long term use also (Haavisto and Paju, 2010).

Few thermal models of FESS can be found in the literature. In (Huynh et al., 2007) for instance, the losses analysis only accounts for the motor losses. Based on results and models collected in the literature concerning thermal modelling of electrical motors and fluid flow modelling, the present paper proposes to predict the losses in the context of low-speed flywheels (4000 rpm), spinning in a low vacuum (5 mbar) and to predict the operating temperature of permanent magnet bearings.
The system considered is designed to store 25 kW h in a 5300 kg steel flywheel, and is schematically represented in Fig. 1: the motor/generator lies outside the enclosure while the permanent magnet bearing is located inside the enclosure, so this study will focus on the thermal behavior of the bearing/flywheel/enclosure sub-system. In this sub-system, the heat sources are the mechanical bearing friction losses, the eddy currents losses in the permanent magnet bearing, and finally the windage losses due to the remaining air in the enclosure. The paper will be divided in two parts : the first part will focus on the evaluation of these losses. The second part will present a finite element model giving the temperature distribution in the system resulting from these losses.

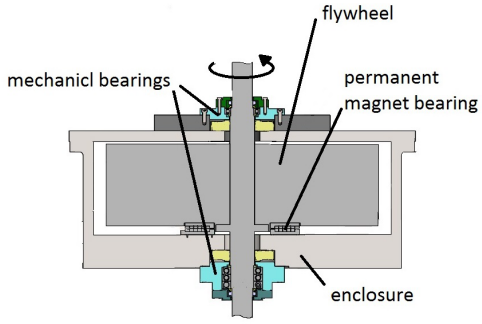

Fig. 1 Considered Flywheel energy storage system

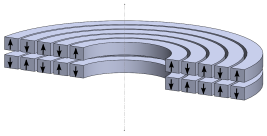

Fig. 2 Permanent magnet thrust bearing

2. Heat sources

2.1. Windage losses

To estimate the windage losses inside the enclosure, given the dimensions of the system and the vacuum level considered, the Navier-stokes equations may be used to predict the behavior of the air inside the enclosure. Indeed, the dimensionless number of Knudsen, which is the ratio between the molecular mean free path length to a representative physical length scale, has been evaluated for the analyzed system. The mean free path is estimated from the molecular density and from the molecular diameter δ, and depends on the pressure P and the temperature T as

$$\Lambda = \frac{k_B T}{\pi \sqrt{2} P \delta^2} \tag{1}$$

For a pressure of 5 mbar, and a temperature of 80 °C , for nitrogen, this mean free path Λ is worth 2.23×10^{-5} m. Taking a representative length of 4 mm, the number of Knudsen is worth $5.6\ 10^{-3}$, which is small enough and means that the Navier-Stokes equations are valid. For systems working at lower pressure, resulting in a larger Knudsen number, one may refer to the article (Reitebuch and Weiss, 1999) in which the flow behavior is predicted for rarefied gas.

In our case, the windage losses can then be evaluated by looking at the solutions of Couette flows, between a fixed wall (the enclosure), and a moving wall at the speed v_{wall} (the flywheel).
At the external radius of the flywheel, the speed is very high, which results in a high Mach number M. Moreover, there is a heat transfer from the flywheel to the enclosure, which means through the air flow around the flywheel. For these two reasons, strictly speaking, the flow may not be modelled by the classical incompressible Couette flow, and a compressible flow should be considered (Liepmann and Roshko, 1957). The problem of a compressible Couette flow is adressed in (Liepmann and Roshko, 1957), supposing that the viscosity μ of the fluid can be represented by a power law $\mu \propto T^{\omega}$. For air, $\omega = 0.76$ is a good approximation. The proposed solution then contains integrals that have to be evaluated numerically, and it becomes much more complicated than considering an incompressible viscous flow.

In this paper, we will consider an incompressible flow and solve the shear stress on the wall τ_{wall} in order to find the losses in the system through:

$$P_{windage} = \tau_{wall} S_{wall} v_{wall}, \tag{2}$$

where S_{wall} is the surface of the wall moving at the speed v_{wall}. The resolution of the laminar incompressible flow is classical, and the turbulent incompressible flow can be solved through the boundary layer theory (Schlichting and Gersten, 1999).

By defining a wall friction velocity $u_\tau = \sqrt{\frac{\tau_{wall}}{\rho}}$, and the Reynolds number $Re_\tau = \frac{\rho h / 2 u_t}{\mu}$, where ρ is the air density, μ is the air dynamic viscosity, and h the distance between the stationary and the moving wall, the shear stress on the wall

can be found.
On one hand, when this Reynolds number is lower than 100, $Re_\tau < 100$, a laminar flow can be considered, and the shear stress is simply worth, if considering cartesian coordinates,

$$\tau_{wall} = \mu \left.\frac{dv}{dy}\right|_{y=h} = \mu \frac{v_{wall}}{h} \tag{3}$$

In laminar conditions, the solutions for a Couette flow between concentric rotating cylinders (Dou et al., 2007) exists, and with cylindrical coordinates, the laminar flow shear stress on the wall is worth:

$$\tau_{wall} = 2\mu \frac{\omega}{1 - (\frac{r_1}{r_1+h})^2} \tag{4}$$

The results for plane and cylindrical coordinates are compared in laminar conditions for our FESS, and Fig. 3 shows that the radius is high enough to neglect the effect of curvature. For the thermal model, the evaluation of the windage losses with the plane coordinates are used.

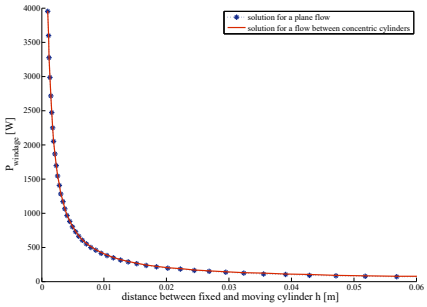

Fig. 3 Comparison of the windage losses at the external surface of the flywheel, at a radius of 0.775 m in laminar conditions, i.e., for a pressure of 5 mbar and a spin speed of 4000 rpm considering the solution for a plane flow and the solution for two concentric cylinders

Finally let us notice that in laminar conditions, for a compressible Couette flow, the solution given in (Liepmann and Roshko, 1957) is evaluated in a simple case, for $\mu \propto T$ ($\omega = 1$), and assuming zero heat transfer. In this case, the shear stress becomes

$$\tau_{wall} = \mu \frac{v_{wall}}{h} \left(1 + Pr \frac{\gamma - 1}{2} M \left(1 - \frac{1}{3}\right)\right) \tag{5}$$

Assuming a Prandtl number Pr of 0.72 for air, a heat capacity ratio γ of 1.4, and the highest Mach number of the system $M = 0.86$, the factor multiplying Eq. (3) is only worth 1.07, which tends to justify the modelization by an incompressible flow.

Let us now consider a turbulent flow, when this Reynolds number is higher than 100, $Re_\tau > 100$ (Schlichting and Gersten, 1999). The shear stress is then calculated by the expression

$$\tau_{wall} = \frac{1}{2} c_f \rho (\frac{v_{wall}}{2})^2, \tag{6}$$

with the skin-friction coefficient c_f which can be found from $c_f = 2(\frac{\kappa}{\ln Re_c} G(\Lambda; D))^2$. In this relation G is a function defined as $\frac{\Lambda}{G} + 2\ln\frac{\Lambda}{G} - D = \Lambda$, in which $\Lambda = 2\ln Re_c$, and D is equal to $2(\ln(2\kappa) + \kappa(C^+ + \bar{C}))$. The Karman constant $\kappa = 0.41$ and coefficient $C^+ = 5$ are universal constants while $\bar{C}$ comes from experimental measurements and is approximatively worth 2.1. The Reynolds number Re_c is formed by v_{wall}: $\rho\frac{v_{wall}h}{\mu}$.
Let us notice that we have considered the surfaces of the walls to be smooth in the windage losses evaluation described above.

For interested readers, the compressible Couette flow is also solved in (Lees and Liu, 1960), and solutions are proposed, with five algebraic equations, depending on the ratio between the Reynolds number and the Mach number Re/M, the squared Mach number M^2 and the ratio of temperature between the fixed and the moving wall. Here again, the equations are much more complicated, and we will only consider the solutions for an incompressible flow in the present paper.

2.2. Induced currents losses

The chosen permanent magnet bearing structure is a thrust bearing consisting in two radial stacks of annular permanent magnets, as illustrated in Fig. 2, which allows to relieve the mechanical bearings of the weight of the flywheel. This reduces the losses of the mechanical bearings and increases their lifetime.

In theory, the chosen permanent magnet bearing structure will generate no losses: the magnetic field is homopolar around the circumference, and thus no eddy currents should be generated. However, in practice, these permanent magnet rings will be assembled by segments, and a small variation in the geometry or in the remanent magnetic flux density from one segment to another is possible. The eddy current losses due to a variation of the magnetization from one segment to another is studied in (Hedlundet al., 2013). Based on the same principle, a FEM has been constructed to evaluate the eddy current losses inside a segment. This model considers one non conducting annular permanent magnet of the stator, which is segmented into 40 pieces. These annular segments are magnetized one out of every two at their maximum remanent flux denisty and the other at their minimum remanent flux density. In this case, the chosen permanent magnets present a remanent flux density of 1.17 T, and the magnet supplier guarantuees a remanent flux density comprised between 1.17 T and 1.22 T. In front of this segmented annular magnet, one single conducting segment of the rotor annular magnet, without magnetization, is spinning at 4000 rpm, and the eddy current losses in this single segment are evaluated. This model is represented in Fig. 4, and the resulting eddy currents in Fig. 5. To have an estimation of the total losses, those losses are multiplied by the number of segments and by the number of annular permanent magnets.

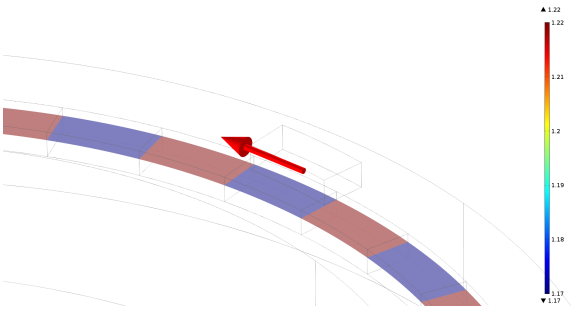

Fig. 4 Finite element model with a ring of annular segments of permanent magnet with a fluctation of the remanent flux density from 1.17 T to 1.22 T and a conductive annular segments spinning above them.

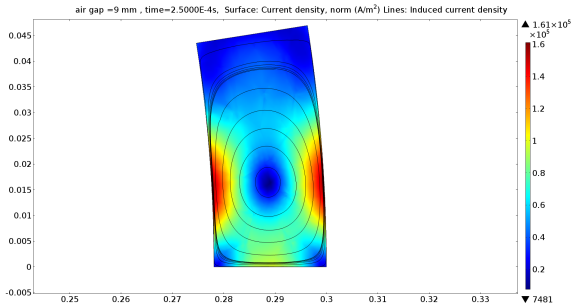

Fig. 5 Finite element model: representation of the eddy currents inside the conducting magnet segment at one fourth of its height while spinning at 4000 rpm, at 9 mm of a segmented annular permanent magnet with a fluctuation of the remanent flux density from one segment to another.

With the spin speed of 4000 rpm, and the remanent flux density varying from 1.17 T to 1.22 T, the eddy currents reach a maximum norm of 1.97×10^5 A mm^{-2}, for the highest considered air gap (10 mm). By way of comparison, in the case when there is no remanent flux density fluctuation from one segment to another, which means that there should be no induced currents at all in the FE model, the maximum eddy current norm is worth 8500 A mm^{-2}, for the smallest considered air gap (4 mm). This leads to the conclusion that the predicted eddy current losses in the FE model come mainly from this remanent flux density fluctuation, and not from the mesh itself.

The eddy current losses in the single conductive segment are represented in Fig. 6 as a function of time for four different airgaps. We see that those eddy current losses vary periodically, with the period directly determined by the spin speed (4000 rpm) and the number of annular segments (40).

However, the considered permanent magnet bearing works at smaller airgaps than those represented in Fig. 6, and the FE model could not be solved for those smaller airgaps, for numerical convergence problems. Supposing that the losses depend on B^2, and that the magnetic flux denisty decreases with the airgap g as $\frac{1}{g}$, then the losses dependance on the airgap is $\frac{1}{g^2}$. The losses in one single segment for smaller airgaps are then extrapolated from the rms values of Fig. 6. This is shown in Fig. 7. At an airgap of 3 mm, the eddy current losses would be around 0.362 W per segment, which results in total losses of around 72 W, in each bearing part, supposing that each bearing part is composed of 5 segmented magnet rings.

In Fig. 8, the windage and the eddy current losses are represented. As the speed of the upper and lower surfaces of the flywheel depend on the radius, these surfaces are divided into discrete annular surfaces having each one a constant speed, and it can be seen on Fig. 8 that the corresponding windage losses are injected into the annular sections. For the

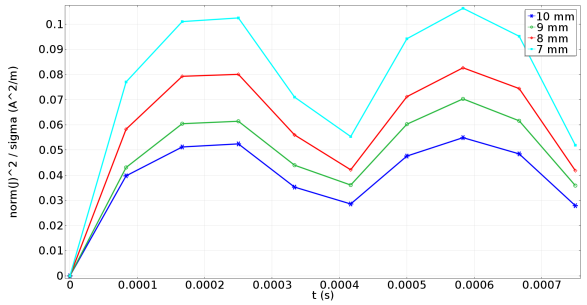

Fig. 6 FE predicted eddy current losses in the single conductive segment, as a function of time, for various air gaps.

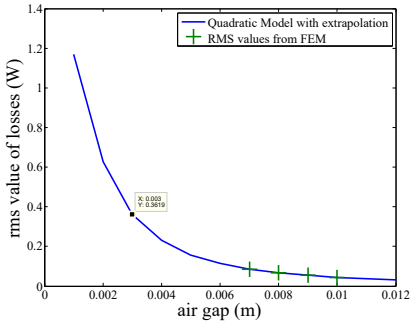

Fig. 7 RMS value of the predicted eddy current losses in one single conductive segment, for various air gaps, and extrapolation.

evaluation of the windage losses in each one of those annular sections, and at the external radius of the flywheel, the air viscosity and the air density, depending on the temperature and on the pressure, are averaged on each one of those volumes.

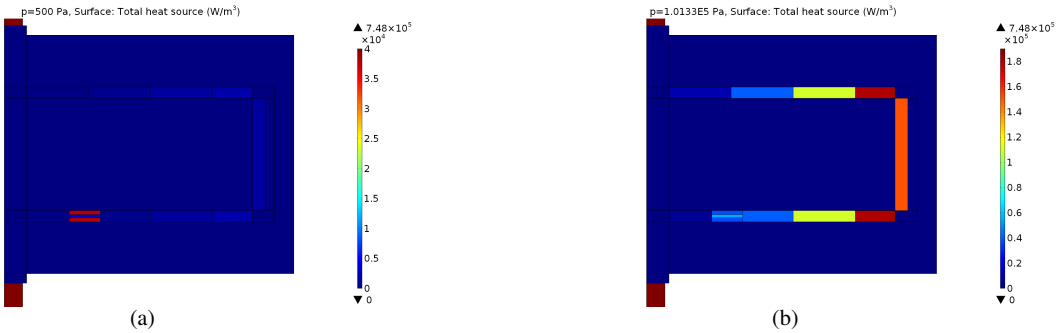

(a) (b)

Fig. 8 Windage and eddy current losses, (a) at a pressure of 5 mbar and (b) at atmospheric pressure.

2.3. Mechanical bearing losses

The mechanical bearing losses are given by the bearing supplier, and are worth 1026 W, at the rate of 25 % in the top bearing and 75 % in the lower bearing.

3. Thermal model

The estimated losses are injected inside the adequate volume inside the FE model which solves the heat equation. This is realized with the software Comsol Multiphysics. Several hypothesis are taken at this stage:

- the flywheel is spinning continuously at its maximum spin speed.
- The thermal behavior of the motor and of the flywheel are considered to be decoupled: there are no thermal exchanges through the mechanical coupling.
- Natural convection is considered at the external boundaries of the system, with a convection factor of 4 $W\,m^{-1}\,K^{-1}$.
- Given that the thermal shrinking between the shaft and the flywheel is partially lost when spinning because of centrifugal forces, a thermal contact resistance between these two elements is considered.
- The losses due to the mechanical bearings are considered to be completely generated inside the shaft, which is more conservative than in reality. The mechanical bearing losses are then injected inside a cylindrical section with a height corresponding to the bearing heigth, and a diameter corresponding to the shaft diameter.
- The vacuum joints are represented by a thermal insulation between the shaft and the enclosure, and are supposed to generate no losses.
- The air thermal conductivity depends on the pressure and on the temperature.
- The convection factors inside the enclosure are determined by experimental formulas (Nerg et al., 2008), and

- the radiation emissivity factor between the enclosure and the flywheel is supposed to be worth $\epsilon = 0.2$.

Let us notice that this model considers a coupling between the windage losses evaluation and the finite element thermal model: indeed the windage losses are calculated by a function of the air density and the air viscosity, which in turn, depend on the temperature. This dependance is implemented in the material library of Comsol multiphysics. For the air, the viscosity μ is expressed as a polynomial function of the temperature T, expressed in Kelvins:

$$-8.38278e-7+8.35717342e-8T-7.69429583e-11T^2+4.6437266e-14T^3-1.06585607e-17T^4, \quad (7)$$

the density ρ is expressed thanks to the law for perfect gas as

$$\frac{P*0.02897}{8.314T}, \quad (8)$$

and the thermal conductivity is also expressed as a polynomial function:

$$(-2.27583562e{-}3{+}1.15480022e{-}4T{-}7.90252856e{-}8T^2{+}4.11702505e{-}11T^3{-}7.43864331e{-}15T^4)*\frac{P}{P_{atm}}. \quad (9)$$

In this last expression, the ratio of pressure has been added to take into account the influence of the pressure on the air conductivity.

3.1. Temperature evaluation in stationary conditions

The FE model is solved in stationary conditions, with a pressure of 5 mbar. The results in Fig. 9 show that the magnets remain in safe temperature conditions, the rotor magnets reach 68 °C, and the stator magnets reach 61.5 °C.

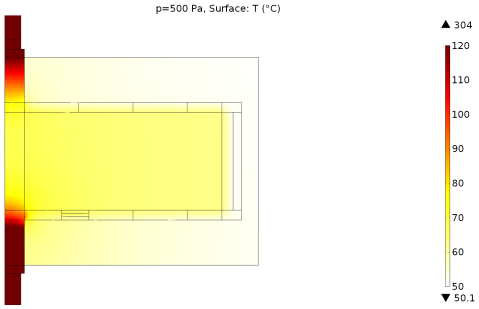

Fig. 9 Temperature distribution inside the vacuum enclosure, at a pressure of 5 mbar.

The geometry of the vacuum enclosure has an influence on the temperature of the magnets, mainly through the windage losses and through the influence of the height of the Couette flow h on these losses. For instance, the windage losses are represented in Fig. 10 when decreasing the radial gap between the external radius of the flywheel and the vacuum enclosure from 4 cm to 4 mm: the windage losses on the external surface of the flywheel increase, and the temperature of the permanent magnet bearing, located on the lower surface of the flywheel, experience a temperature increase, as shown in Fig. 11.

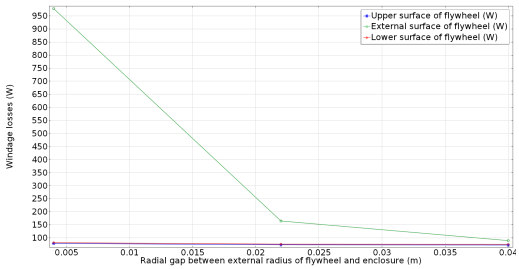

Fig. 10 Windage losses evolution with a decrease of the radial gap between the external radius of the flywheel and the vacuum enclosure.

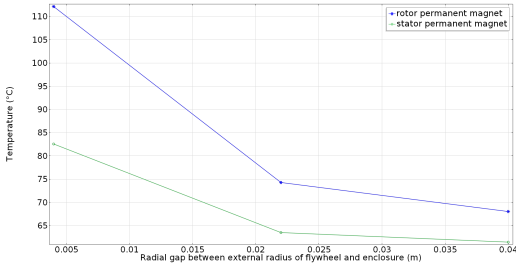

Fig. 11 Permanent magnet maximum temperature evolution with a decrease of the radial gap between the external radius of the flywheel and the vacuum enclosure.

The evolution of the permanent magnet temperature can also be studied when varying the flywheel spin speed. Up to now, a constant 4000 rpm spin speed has been considered. The windage losses depend on this speed through Eqs. (3) or (6). We can also suppose that the eddy current losses are proportionnal to the square of the spin speed. The slight increase of the convection factor between the flywheel and the enclosure is not taken into account in this simulation. Indeed, as long as the Couette flow remains laminar, which is the case here, the heat flux taking place thanks to the convection is much smaller than the heat flux taking place through radiation. Finally, the temperature increase, in stationary condition, when the constant spin speed of the flywheel is increased, as shown in Fig. 12.

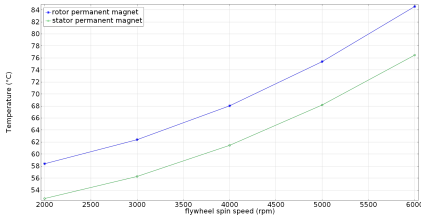

Fig. 12 Permanent magnet maximum temperature evolution with the flywheel spin speed.

The influence of other parameters can also be studied. Indeed, as explained in the section describing the windage losses evaluation, the assumption is made that an incompressible Couette flow may be considered, which is not the case everywhere in the system. For the eddy current losses, the worst case has been considered: the remanent flux density varies at each segment. Other parameters are not very well known, like the convection factors inside the enclosure, the emissivity factor, the thermal contact resistance between the shaft and the flywheel. Also, the convection factor outside the enclosure could easily be increased by adding some cooling fins. For these reasons, it is interesting to look at the sensitivity of the temperature prediction in stationary conditions to thoses parameters. Those results are represented in Fig. 13. The parameters with the highest influence are the windage losses evaluation, and mainly the external convection factor.

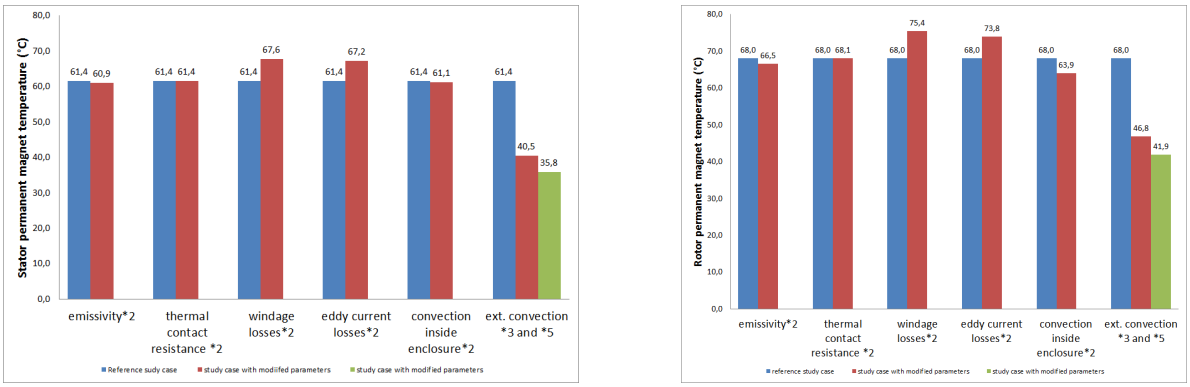

Fig. 13 Permanent magnet maximum temperature sensitivity to various model parameters.

3.2. Temperature evaluation in transient conditions, in case of vacuum loss

The rise of the temperature of the permanent magnets in case of a sudden loss of vacuum, while the spin speed of the flywheel is kept constant at 4000 rpm, has also been modelled, and the results are presented in Fig. 14. The time evolution of permanent magnet temperature shows a decrease of the rotor permanent magnets, and an increase of the stator permanent magnets during the first minutes, thanks to the better heat transfer in the air at atmospheric pressure than at low pressure. Then, both parts of the permanent magnet bearing undergo a slow increase of temperature, thanks to the high inertia of the flywheel: after 180 min, their temperature reaches 124 °C. Indeed, the product of the specific heat of steel and the weight of the flywheel is very high: $2.438 \times 10^6\,\mathrm{J\,K^{-1}}$.

4. Conclusion

The first focus of this paper is the evaluation of the windage losse inside a low vacuum enclosure. The windage losses

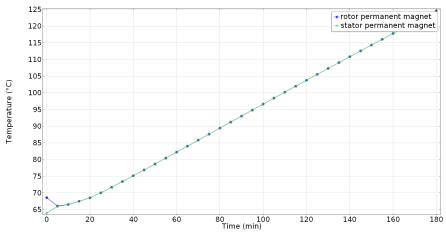

Fig. 14 Permanent magnet maximum temperature evolution with time, in case of a sudden loss of vacuum.

are evaluated by an incompressible Couette flow approximation, even though the tangential speed of the flywheel is very high and the presence of heat exchange through the air. The eddy current losses are evaluated by a FE electro-mechanical model, and an extrapolation, for a case in which the remanent flux density varies at each annular segment of permanent magnet.

Based on the evaluation of these losses, a FE thermal model of the system is build. The results show that, for the configuration of FESS presented in this paper, the temperatures inside the permanent magnet bearing remains at acceptable levels.

Further modelling work could concern a better evaluation of the windage losses, either by models of a compressible Couette flow, either by CFD models. The thermal model could also be improved by injecting the mechanical bearing losses inside the mechanical bearings, instead of directly inside the shaft. However, the present model is sufficient to have an upper bound of the temperature inside the permanent magnets, at a design stage. At a further stage, experimental measurements of the temperature inside the system will be needed.

References

H.-S. Dou, B.C. Khoo, K.S. Yeo, Energy Loss Distribution in the Plane Couette Flow and the Taylor-Couette Flow between Concentric Rotating Cylinders, International Journal of Thermal Science, Vol. 46, pp 262-275, 2007.

J. Friebe, P. Zacharias, Review of Magnetic Material Degradation Characteristics for the Design of Premagnetized Inductors, IEEE Transactions on Magnetics, Vol. 50(3), March 2014, p 4003809.

G. Genta, Kinetic Energy Storage: an Ideal Application for Magnetic Bearings, Proceedings of ISMB14, 2014.

M. Haavisto, M. Paju, Time-Dependent Demagnetization in Sintered NdFeB Magnets, Proceedings of the 21 st Workshop on Rare-Earth Permanent Magnets and their Applications, 2010, pp224-226.

M. Hedlund, J. Abrahamsson, J. Jose Perez-Loya, J. Lundin, H. Bernhoff, Passive Axial Thust Beairng for a Flywheel Energy Storage System, Proceedings of First Brazilian Workshop on Magnetic Bearings, 2013.

C. Huynh, L. Zheng, P. McMullen, Thermal Performance Evaluation of a High-Speed Flywheel Energy Storage System, Industrial Electronics Society, 2007. IECON 2007. 33rd Annual Conference of the IEEE, Nov. 2007, pp 163-168.

H. W. Liepmann, A. Roshko, Elements of Gasdynamics, John Wiley & Sons, 1957.

L. Lees, Ch.-Y. Liu, Kinetic Theory Description of Plane, Compressible Couette Flow, Research report, Guggenheim aeronautical laboratory, California Institute of Technology, Sept. 1960.

J. Nerg, M. Rilla, J. Pyrhnen, Thermal analysis of Radial-Flux electrical machines with a high power density, IEEE Transactions on Industrial Electronics, Vol. 55 (10), pp3543-3555, Oct. 2008.

D. Reitebuch, W. Weiss, Application of High Momentum Theory to Plane Couette Flow, Continuum Mech. Thermodyn., Vol. 4, pp 217225, 1999.

S. Sabihuddin , A. E. Kiprakis, M. Mueller, A Numerical and Graphical Review of Energy Storage Technologies, Energies 2015, 8(1), pp 172-216; doi:10.3390/en8010172 .

H. Schlichting, K. Gersten, Boundary Layer Theory, Springer, 1999.

M. Van Beneden, V. Kluyskens, B. Dehez, Comparison between optimized geometries of permanent magnet ironless load compensators, Proceedings of ISEF 2015, Valencia, Spain, September 2015.

5. Acknowledgement

This work was supported by the Walloon Region.